

The Nature of Kikuchi Lines in the Bragg Case in Reflexion High-Energy Electron Diffraction

BY SHIZUO MIYAKE*

Institute for Solid State Physics, University of Tokyo, Roppongi-7, Minato-ku, Tokyo, Japan

KAZUNOBU HAYAKAWA

Central Research Laboratory, Hitachi Ltd, Kokubuniji, Tokyo 185, Japan

TAKAAKI KAWAMURA AND YOSHI-HIKO OHTSUKI

Department of Physics, Waseda University, Nishi-Ohkubo 4, Shinjuku-ku, Tokyo, Japan

(Received 9 January 1974; accepted 30 June 1974)

The behaviour of the Kikuchi lines parallel to the shadow edge, which are formed under diffraction conditions in the Bragg case, is experimentally studied for zincblende (ZnS), MgO and rock salt. A line of this group generally has an asymmetric intensity profile across it. Sometimes it shows contrast reversal from an excess appearance in the central range to a defect appearance in the side ranges along the line. These peculiarities become noticeable with the increase in the glancing angle of the incident beam with the crystal surface. It is pointed out that theoretically the form of the line term in the intensity formula for Kikuchi patterns in the Bragg case differs from that in the Laue case. The variation of the line profile, including the effect of contrast reversal, takes place by the change in the intensity formula, in the ratio of the band term to the line term, depending on the scattering vector appropriate to the inelastic electron scattering involved. By assuming approximate forms for the scattering factors for Kikuchi patterns, the observed results are qualitatively explained.

1. Introduction

The contrast reversal of Kikuchi bands is a characteristic phenomenon in high-energy electron diffraction (HEED), which takes place depending on the scattering angle, the glancing angle (in reflexion experiments), the crystal thickness (in transmission experiments), and the electron energy (Shinohara & Matsukawa, 1933; Pfister, 1953; Alam, Blackman & Pashley, 1954). This phenomenon has also been dealt with in a number of recent experimental and theoretical investigations (Ishida, 1970, 1971; Nakai, 1970; Okamoto, Ichinokawa & Ohtsuki, 1971; Chukhovskii, Alexanjan & Pinsker, 1973; Arii, 1973).

So far, however, observations of a similar effect in Kikuchi lines seem to be few. In addition, the theoretical studies given in the past are mostly for Kikuchi patterns in the Laue case, while those for Kikuchi patterns in the Bragg case can be found only in a short discussion given by Takagi (1958) and a recent treatment by Kawamura, Ichikawa & Goldsztaub (1973).

In the above, the separation of the diffraction conditions into the Laue case and the Bragg case is given for the inelastically scattered electrons contributing to Kikuchi patterns, in terms of the two-wave approximation (Fig. 1). Kikuchi lines found in a transmission pattern from a thin crystal specimen are exclusively those in the Laue case, while those in the Bragg case may appear in a reflexion pattern (RHEED pattern)

obtained from a cleavage face of a crystal. Particularly, the Kikuchi lines parallel to the shadow edge, which are caused by the lattice plane parallel to the crystal surface, are obviously in the Bragg case over their whole line length. Hereafter, these Kikuchi lines are called the 'H. K. lines', as an abbreviation for 'horizontal Kikuchi lines'.

In many cases the H.K. lines appear to be similar to ordinary Kikuchi lines [*e.g.*, Fig. 5(a)]. In their experimental observations, however, the present authors noticed that, as a characteristic phenomenon, the H.K. line occasionally shows contrast reversal, from an excess appearance in the central range to a defect appearance in the side ranges along the line length.* In addition, it was found that each H.K. line generally has an asymmetric intensity profile more or less across it. As these features are thought to be due to the peculiarity of Kikuchi lines in the Bragg case, the behaviour of the H.K. lines has been investigated experimentally as well as theoretically in more detail in the present paper.

2. Experimental

The observations of RHEED patterns were performed on cleavage faces of zincblende (ZnS), magnesium oxide (MgO) and rock salt (NaCl), with the electrons

* It appears that Professor K. Shinohara had already noticed this effect in the course of his pioneering work on Kikuchi patterns in the early 1930's (private communication through Professor K. Kohra). One of the present authors (S.M.) independently became aware of this effect some years later.

* Home address: 2-29-1 Minami-Ogikubo, Suginami-ku, Tokyo 167, Japan.

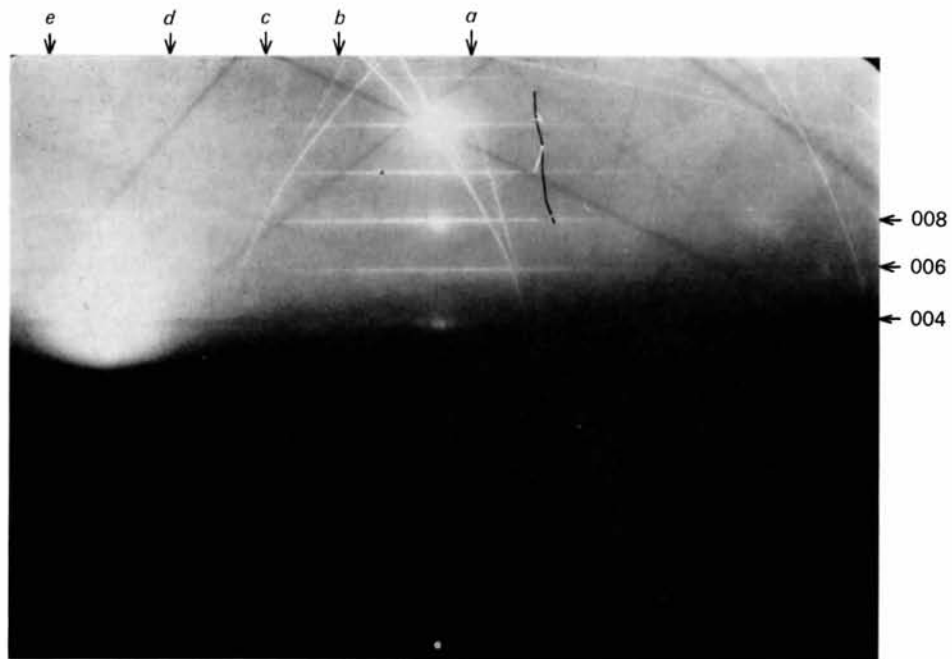


Fig. 2. RHEED pattern (100 keV) from the (001) surface of MgO for an azimuth deviated about 10° from [110]. α (glancing angle) = 2.7° .

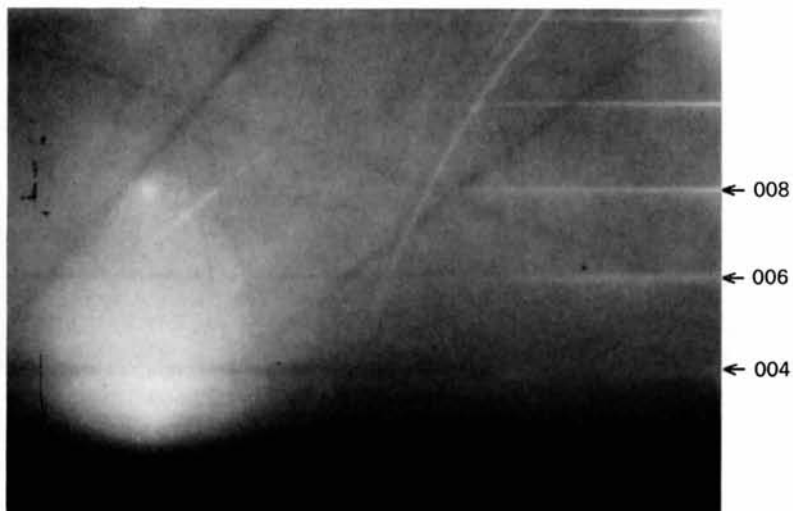


Fig. 3. Magnification of a part of Fig. 2. Contrast reversal can be observed for the 004, 006 and 008 Kikuchi lines.

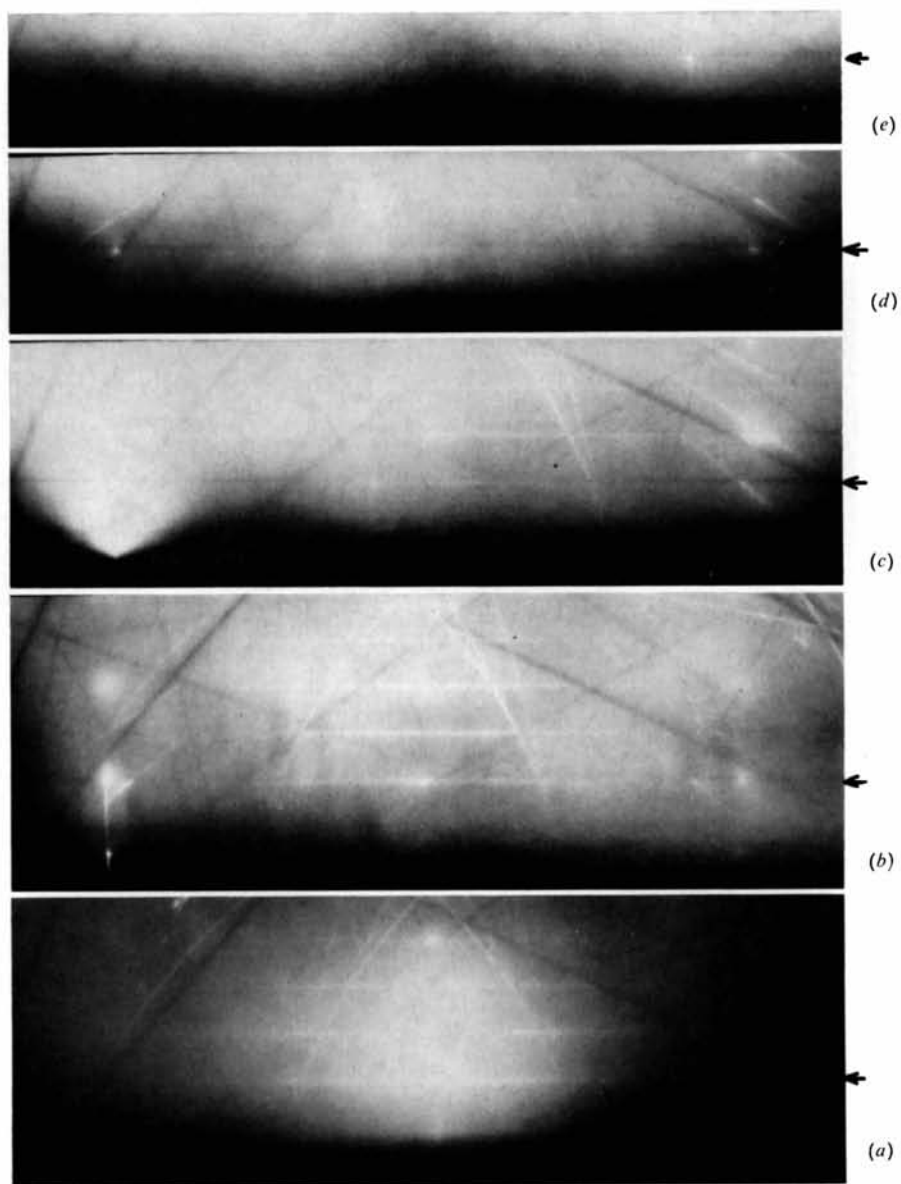
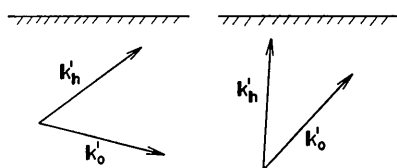


Fig. 5. Series of RHEED patterns (100 keV) from MgO for an azimuth deviated about 10° from [110]. (a), (b), (c), (d) and (e) correspond to $\alpha = 1.7, 3.2, 3.7, 4.2$ and 4.7° respectively. The arrows indicate each position of the 006 H.K. line.

of 100 keV used throughout. It is generally inevitable that the H.K. lines interfere with many Kikuchi lines and bands which cross them, sometimes severely for certain crystal azimuths. Therefore, favourable azimuths were selected so that the H.K. lines could be observed without serious interference.

The intensity profile across an H.K. line was measured by photometry on the diffraction photograph; the light spot used was of a size $30 \times 300 \mu\text{m}$ with the longer side set parallel to the line. The photometer curve for a RHEED pattern generally has a steep gradient down towards the shadow edge, and this



(a) Bragg case (b) Laue case

Fig. 1. Directions of the wave vectors k_o and k_h relative to the crystal surface, for the plane-wave components of a two-term Bloch function representing an inelastically scattered electron spot in the crystal.

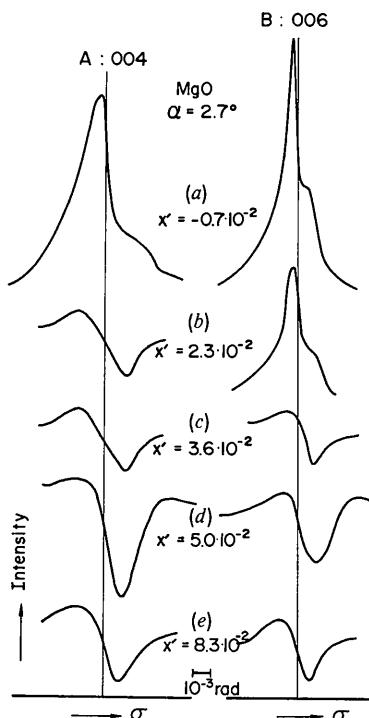


Fig. 4. Photometer curves of the intensity profiles on an arbitrary scale of the 004 (A) and 006 (B) H.K. lines in the pattern from MgO shown in Figs. 2-3 along the coordinate σ which is perpendicular to the lines and increases with the scattering angle. (a), (b), (c), (d) and (e) correspond to the azimuthal positions concerned as indicated by the arrows in Fig. 1. $x' = x/L$, x , the distance along the H.K. line from its central position, L , the camera length.

makes it rather difficult to separate the genuine profile of the line from the background without ambiguity. In this study, the background in the limited range beneath the H.K. line concerned was approximated either by a straight line or by a spherical arc, such that the subtraction procedure will give an H.K. line profile with reasonable levels and forms at the two tail ends.

3. Contrast reversal and asymmetric profiles of H.K. lines

Fig. 2 shows a reflexion pattern from the cleavage face (001) of a MgO crystal, for an azimuth deviating about 10° from [110] and for glancing angle $\alpha = 2.7^\circ$. Fig. 3 is a magnification of a part of Fig. 2. In these figures the contrast reversal is clearly seen for the H.K. lines 004, 006, and 008.

Fig. 4 shows the intensity profiles of the H.K. lines 004 and 006 obtained for the azimuthal positions indicated in Fig. 2. The ordinates of the figures stand for the intensity, with floating origins, on a scale which is arbitrary but common for all the profiles. The abscissae correspond to the coordinate σ with respect to an axis perpendicular to the H.K. lines towards higher scattering angles (*i.e.* in the upward direction across the line); the lateral positions of the profiles have been relatively adjusted to one another as reasonably as possible by visual inspection of the photographs. Fig. 4 clearly shows that an H.K. line generally has an asymmetric intensity profile. It should be noted that even a seemingly normal excess contrast in an H.K. line in its central range already bears some asymmetric feature, as seen in Fig. 4A(a) and B(b). The features of the H.K. lines from MgO as shown in Figs. 2-4 were similarly observed in RHEED patterns from the (011) face of zincblende and the (001) face of rock salt. They can be summarized as follows:

The asymmetric intensity profile of an H.K. line consists of a combination of two parts, one the excess part located on the downside (with a lower value of σ), and the other the defect part on the upside (with a higher value of σ). With increase in the distance x along the line from its central position, the excess part gradually diminishes both in peak height and width, while the defect part increases both in defect depth and width. The contrast reversal along an H.K. line is a result of such a variation in the asymmetric profile with x . In this variation the difference between σ_e , the coordinate corresponding to the excess intensity maximum, and σ_d , that corresponding to the defect minimum, does not substantially change. Therefore, when an H.K. line with excess contrast in its central range changes to one with defect contrast in the side ranges, the latter is geometrically not in line with the former, but a finite step corresponding to $\sigma_d - \sigma_e$ exists between them, as can be clearly seen in Fig. 3.

Between the extreme ranges of the contrast along an H.K. line, there is a transitional region where the excess and defect parts coexist with equal weight, for

which the intensity profile assumes typically an asymmetric form as seen in Fig. 4A(c) and B(c).

4. Dependence on the glancing angle

When the glancing angle α is as small as $0.25 \sim 0.5^\circ$ most of the H.K. lines are found to be rather weak. In general an H.K. line $00h$ has the strongest excess contrast when the specular spot comes to lie on it to satisfy the Bragg condition $00h$. The asymmetric feature and the contrast reversal of the same H.K. line begin to become increasingly noticeable when the specular spot after having crossed this line deviates upwards by a further increase in α .

Fig. 5 shows a series of RHEED photographs from a MgO crystal taken at a slightly different crystal azimuth from that for Fig. 2, for various values of α . In these figures, one may note that the contrast reversal of the H.K. lines takes place as if it advanced from lower-order lines to higher-order ones with the increase in α . For instance, the contrast reversal, which cannot be found in Fig. 5(a) for $\alpha = 1.7^\circ$, becomes evident in the lines 004, 006 and 008 in Fig. 5(b) for $\alpha = 3.2^\circ$, and also in the line 0,0,10 in Fig. 5(c) for $\alpha = 3.7^\circ$. As to 004, it is only in (a) that this line shows any excess contrast in the central range. In (d) for $\alpha = 4.2^\circ$ and (e) for $\alpha = 4.7^\circ$, particularly in the latter, the excess part of the line 006 almost vanishes over its whole length.

The trend mentioned above can be summarized in terms of the *transitional boundary*, which is a band (or curve) formed by connecting the transitional regions on each H.K. line. This boundary divides the diffraction pattern into the excess and the defect areas with respect to H.K. lines, as illustrated in Fig. 6. By inspecting Fig. 5, it is known that the form and the location of the transitional boundary relative to the specular spot S are almost independent of α in the range of α from 3.20 to 4.70° . This implies that, as α increases, the transitional boundary moves upwards together with the specular spot S located at the scattering angle 2α ,* with speed twice that of the shadow edge and of the Kikuchi pattern system. Thus, the contrast reversal advances from lower to higher-order H.K. lines, as these lines are successively included in the defect area outside the transitional boundary. This boundary can be approximated over its greater part by two straight bands forming an obtuse angle of about 120° , as illustrated in Fig. 6. The transitional boundary for zincblende was found to be almost the same.

The physical meaning of the transitional boundary may be understood as follows. Fig. 7 shows schematically the cross section of the dispersion surface in the plane perpendicular to the crystal face (001) of an f.c.c. crystal; the small circles mark the vertex regions proper to the diffraction conditions on 004, 006, 008, etc. If

the initial state $\psi_{\mathbf{k}_0}$ ($\mathbf{k}_0 = \vec{AO}$), consisting of a single plane wave, undergoes an inelastic transition to another state $\psi_{\mathbf{k}'_0}$ ($\mathbf{k}'_0 = \vec{BO} = \mathbf{k}_0 + \mathbf{q}$, $\mathbf{q} = \vec{BA}$) relevant to a tie-point B lying in the region of one of the small circles, say that for 006, then the inelastic transition $A \rightarrow B$ contributes to formation of the Kikuchi line 006.

Now, we consider in Fig. 6 the mirror image of the pattern above the shadow edge; thus the \mathbf{q} boundary is the mirror image of the transitional boundary, D is the direct spot due to the incident beam, and the lines 004, 006, etc. correspond geometrically to those Kikuchi lines which are not actually observable. It is obvious that the wave vectors \mathbf{k}_0 , \mathbf{k}'_0 and \mathbf{k}'_{006} ($= \mathbf{k}'_0 + \mathbf{h}_{006}$; \mathbf{h}_{006} , the reciprocal vector for 006) in Fig. 7 correspond to the points D , E and F in Fig. 6, respectively, and \vec{DE} corresponds to \mathbf{q} . The \mathbf{q} boundary, therefore, represents a boundary such that when the top of \mathbf{q} is located inside or outside this boundary, the inelastic scattering concerned gives an H.K. line with excess or defect contrast, respectively. This role of the \mathbf{q} boundary fixed relative to the direct spot D is the same as that of the transitional boundary fixed relative to the specular reflexion S in the actual diffraction pattern. It should be noted that the location of the tie-point B and therefore the vector \mathbf{q} may become imaginary in the Bragg case under a certain condition, even without absorption.

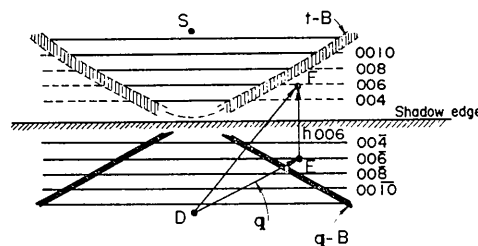


Fig. 6. A sketch of Fig. 2, illustrating the transitional boundary ($t-B$). The part below the shadow edge is the mirror image of that above this line. D , the direct spot; S , the specular reflexion; \mathbf{q} boundary ($q-B$), the mirror image of the transitional boundary.

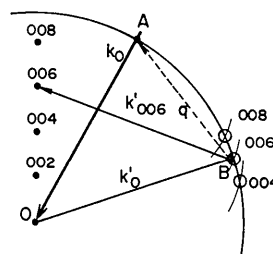


Fig. 7. Dispersion surface relevant to the generation of the H.K. lines, appropriate to the case of MgO. The tie point A corresponds to the initial state and B to the final state.

* In Fig. 5 the specular spot is only seen in (a) and (b), because of the limited size of the photographic film.

5. Theoretical basis

As is well known, an ordinary Kikuchi line in the Laue case also has an asymmetric character owing to the so-called band term (Kainuma, 1955; Takagi, 1958), but this term is known to become relatively less significant as the location of the line pair concerned deviates more from the direct spot corresponding to the incident beam. The asymmetric feature of an H.K. line, on the other hand, becomes increasingly conspicuous under similar circumstances, which in this case are due to the increase in the glancing angle α . This contrast indicates that the asymmetric profiles as well as the contrast reversal of the H.K. lines are of a nature peculiar to them.* In the previous paper, Kawamura *et al.* (1973) theoretically dealt with the Kikuchi patterns in the Bragg case on the basis of the two-wave approximation for a semi-infinite crystal involving absorption. Their theory is briefly outlined below.

According to the formal theory of scattering (Messiah, 1965; Wu & Ohmura, 1962), the intensity J_0 of the Kikuchi pattern is given, in the distorted-wave Born approximation, by

$$J_0 d\Omega \propto \frac{2\pi}{\hbar} \sum_{n \neq 0} |\langle \psi_{\mathbf{k}'}^{(-)} | a_n | H' | \psi_{\mathbf{k}_0}^{(+)} | a_0 \rangle|^2 \rho(\mathbf{K}') \quad (1)$$

where a_n is the wave function of the n th excited state of the crystal, H' represents the part of the Hamiltonian responsible for the inelastic scattering and $\rho(\mathbf{K}')$ is the state density of the final states for a specified vector \mathbf{K}' . (Refer also to Takagi (1958) and Okamoto *et al.* (1971).) We put $|\psi_{\mathbf{k}_0}^{(+)}\rangle = \exp(2\pi i \mathbf{K}_0 \mathbf{r})$ corresponding to the incident wave $\exp(2\pi i \mathbf{k}_0 \mathbf{r})$ at the crystal surface, which is assumed to be remote from any Bragg condition, where $|\mathbf{K}_0| = |\mathbf{k}_0| + m e V_0 / \hbar^2 |\mathbf{k}_0|$, and V_0 is the inner potential. If we are concerned with the inelastically scattered wave emerging from the crystal surface with wave vector \mathbf{k}' , then the wave function of the final state in equation (1) is of the form

$$\langle \psi_{\mathbf{k}'}^{(-)} | = \psi_{\mathbf{k}'}^{(-)} = \psi_{-\mathbf{k}'}^{(+)} = \sum_{\mathbf{h}} C_{\mathbf{h}} \exp(-2\pi i \mathbf{K}_{\mathbf{h}}' \mathbf{r}) \quad (2)$$

which is the 'reciprocal wave' used successfully by Kainuma (1955) in his theory of Kikuchi patterns, where \mathbf{K}' is a wave vector whose tangential component to the crystal surface is equal to that of \mathbf{k}' , $\mathbf{K}_{\mathbf{h}}' = \mathbf{K} - \mathbf{h}$ and \mathbf{h} is the reciprocal-lattice vector.

In the two-wave approximation in the Bragg case for a semi-infinite crystal, only one tie-point is permitted on the dispersion surface (Takagi, 1958; Kohler,

* The peculiarity of the H.K. lines has long been overlooked, probably because the angular range of the glancing angle α has been limited at a maximum of the order of only 5° with the usual RHEED setting, owing to a limited size of photographic film, and also because a range $\alpha \approx 1 \sim 2^\circ$ is used in most RHEED practice. As seen in Fig. 5 the peculiarity of the H.K. lines becomes noticeable only when α is larger than about 2° . In fact, it is only on a wide fluorescent screen that one can observe the entire aspect of the defect H.K. lines extending over a considerable range in the pattern.

1933), which gives the wave field accompanying the electron flow directed inwards with respect to the crystal surface. Assuming the symmetrical Bragg case, we have

$$C_0 = 1, \quad C_{\mathbf{h}} = -\frac{1}{1+ik} (W + ig + \sqrt{B}), \quad (3)$$

where $\sqrt{B} = \text{Re}\sqrt{B} + i \text{Im}\sqrt{B}$ and

$$\begin{aligned} \text{Re}\sqrt{B} = & \pm \frac{1}{\sqrt{2}} [(W^2 - 1 - g^2 + k^2) \\ & + \sqrt{(W^2 - 1 - g^2 + k^2)^2 + 4(gW - k)^2}]^{1/2}; \quad (4) \\ & + : gW - k \geq 0, \quad - : gW - k \leq 0 \end{aligned}$$

$$\begin{aligned} \text{Im}\sqrt{B} = & \frac{1}{\sqrt{2}} [-(W^2 - 1 - g^2 + k^2) \\ & + \sqrt{(W^2 - 1 - g^2 + k^2)^2 + 4(gW - k)^2}]^{1/2}. \end{aligned}$$

W , the 'Selektionsfehler', is defined in such a way that it increases with the increase of the angle between \mathbf{k}' and the crystal surface; g and k , the quantities responsible for the normal and abnormal absorption, respectively, are given by

$$g = C_{00}^i / |U_{\mathbf{h}}^r| \quad \text{and} \quad k = C_{0\mathbf{h}}^i / |U_{\mathbf{h}}^r|, \quad (5)$$

where $U_{\mathbf{h}}^r$, C_{00}^i are the potential terms [refer to Kawamura *et al.* (1973)]. The substitution of the wave function into equation (1) gives the intensity of an H.K. line

$$\begin{aligned} J_0 \propto & S(\mathbf{Q}, \mathbf{Q}) + \frac{1}{1+k^2} [(W + \text{Re}\sqrt{B})^2 \\ & + (g + \text{Im}\sqrt{B})^2] S(\mathbf{Q}_{\mathbf{h}}, \mathbf{Q}_{\mathbf{h}}) \\ & - \frac{2}{1+k^2} [(W + \text{Re}\sqrt{B}) + k(g + \text{Im}\sqrt{B})] S(\mathbf{Q}, \mathbf{Q}_{\mathbf{h}}), \quad (6) \end{aligned}$$

where $\mathbf{Q} = \mathbf{K}' - \mathbf{K}_0$ and $\mathbf{Q}_{\mathbf{h}} = \mathbf{Q} - \mathbf{h}$; $S(\mathbf{Q}, \mathbf{Q})$, $S(\mathbf{Q}_{\mathbf{h}}, \mathbf{Q}_{\mathbf{h}})$ and $S(\mathbf{Q}, \mathbf{Q}_{\mathbf{h}})$ are quantities corresponding to the structure factors for Kikuchi patterns (Kainuma, 1955); $\mathbf{Q}_{\mathbf{h}}$ is essentially the same as the vector \mathbf{q} introduced in § 4.

6. Theoretical results

The first term of J_0 in equation (6) corresponds to the background intensity. The second and third terms may be called the line and band terms, respectively, following the names of the corresponding terms in the Laue case. It should be noted that the line term in the Bragg case contains the factor $S(\mathbf{Q}_{\mathbf{h}}, \mathbf{Q}_{\mathbf{h}})$ only, instead of $S(\mathbf{Q}_{\mathbf{h}}, \mathbf{Q}_{\mathbf{h}}) - S(\mathbf{Q}, \mathbf{Q})$ in the Laue case.

In the Laue case, because of its form proportional to $S(\mathbf{Q}_{\mathbf{h}}, \mathbf{Q}_{\mathbf{h}}) - S(\mathbf{Q}, \mathbf{Q})$, the line term vanishes at the symmetric condition fulfilling $|\mathbf{Q}| = |\mathbf{Q}_{\mathbf{h}}|$, and its value rapidly increases with the increase in the ratio $|\mathbf{Q}|/|\mathbf{Q}_{\mathbf{h}}|$ from unity. Therefore, the ratio of the line term to the band term, which is represented by

$$b_L = \frac{S(\mathbf{Q}, \mathbf{Q}_h)}{S(\mathbf{Q}_h, \mathbf{Q}_h) - S(\mathbf{Q}, \mathbf{Q})}, \quad (7)$$

varies over a wide range with \mathbf{Q} and \mathbf{Q}_h . In the Bragg case, on the other hand, the change of the corresponding ratio,

$$b_B = \frac{S(\mathbf{Q}, \mathbf{Q}_h)}{S(\mathbf{Q}_h, \mathbf{Q}_h)}, \quad (8)$$

is not so conspicuous as in the Laue case. Nevertheless, the fine structure of the intensity profile given by J_0 in equation (6) undergoes a significant variation depending on b_B .

The function $S(\mathbf{Q}, \mathbf{Q}_h)$ has been theoretically calculated for the core-electron excitation (Kainuma, 1955; Okamoto *et al.*, 1971) as well as for the phonon excitation (Takagi, 1958; Okamoto *et al.*, 1971) for the transmission case. In the reflexion case for, *e.g.*, the phonon excitation, $S(\mathbf{Q}, \mathbf{Q}_h)$ can approximately be given in the form

$$\begin{aligned} S(\mathbf{Q}, \mathbf{Q}_h) \propto & \frac{1}{\mu} \frac{1}{Q^2} \frac{1}{Q_h^2} \left[\sum_{\nu} f_{\nu}^*(\mathbf{Q}) - Z \right] \\ & \times \left[\sum_{\nu} f_{\nu}(\mathbf{Q}_h) - Z \right] \\ & \times \{ \exp[-M(\mathbf{h})] - \exp[-M(\mathbf{Q}) - M(\mathbf{Q}_h)] \} \end{aligned} \quad (9)$$

where $f_{\nu}(\mathbf{Q})$ is the Compton scattering factor, Z the atomic number, $\exp[-M(\mathbf{h})]$, *etc.* are the Debye-Waller factors and μ the absorption coefficient which is defined by

$$\mu = |U_h^*| (g + \text{Im } \sqrt{B}) / K_0^2, \quad (10)$$

where the term $\text{Im } \sqrt{B}$ describes the anomalous absorption for $W \lesssim -1$ and the anomalous transmission for $W \gtrsim 1$. Thus the part of J_0 excluding the background term is given by

$$J_0' \propto \frac{(W + \text{Re } \sqrt{B})^2 + (g + \text{Im } \sqrt{B})^2 - 2b_B[(W + \text{Re } \sqrt{B}) + k(g + \text{Im } \sqrt{B})]}{g + \text{Im } \sqrt{B}}. \quad (11)$$

Fig. 8 shows an example of the intensity profiles J_0' calculated from (11) for the values $b_B = 0, 0.50, 0.75$ and 1.0 , assuming the absorption parameters $g = 0.2$ and $k = 0.1$; the ordinate stands for the intensity on an arbitrary scale and the abscissa corresponds to W , which is linear in the coordinate σ defined in § 3 in the direction across the H.K. lines. Fig. 8 indicates that the intensity profile with the excess contrast for small b_B begins to bear an asymmetric character with the increase in b_B , and that the asymmetric profile as well as the contrast reversal of the H.K. lines as experimentally observed is due to the change in b_B . In other words, the peculiar features of the H.K. lines may be enhanced when the band term, accompanied by a deep negative region in the range $0 < W \leq 1$, becomes comparable with the line term which is positive throughout.

Because the dependence of $S(\mathbf{Q}, \mathbf{Q}_h)$ on \mathbf{Q} and \mathbf{Q}_h is approximately similar for both the phonon excitation

and the core excitation, the behaviour of the H.K. lines with the change of b_B may be discussed on the basis of the form (9). If, for simplicity, the temperature dependence due to the Debye-Waller factors, and the \mathbf{Q} and \mathbf{Q}_h dependence of the Compton scattering factors are neglected, b_B is approximately given by

$$b_B = \frac{Q_h^2}{Q^2} = \frac{(Q-h)^2}{Q^2}. \quad (12)$$

On the basis of equation (12), b_B can be expressed in terms of x , or the distance along an H.K. line from its central position as defined in § 3, and the glancing

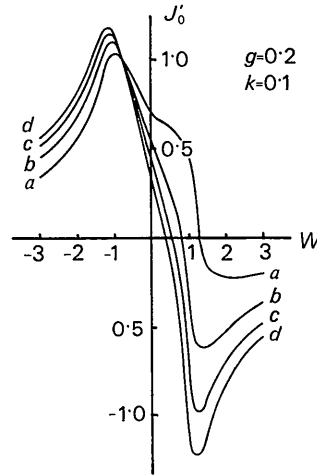


Fig. 8. The intensity profiles J_0' calculated from equation (11) for $g = 0.2$ and $k = 0.1$. Curves *a*, *b*, *c* and *d* correspond to $b_B = 0.25, 0.50, 0.75$ and 1.0 respectively. The ordinate, the intensity on an arbitrary scale, and the abscissa, W (Selektionfehler, which is linear in the coordinate σ across the H.K. lines). Each profile is normalized at $W = -0.75$.

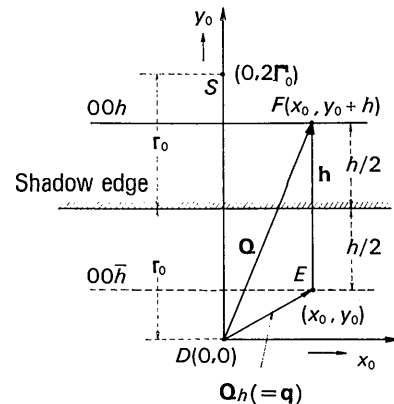


Fig. 9. Geometry in an RHEED pattern. D , the direct spot; S , the specular reflexion, $\Gamma_0 = K\alpha$ (α , the glancing angle, K , the wave number) is equal to the normal component of \mathbf{k}_0 to the crystal surface. $x_0 = K(x/L)$, x , the distance along the Kikuchi line from its central position, L , the camera length.

angle α . Using the approximations $\mathbf{k}_0 = \mathbf{K}_0$ and $\mathbf{k}'_0 = \mathbf{K}'_0$, we obtain

$$b_B = 1 - \frac{2\Gamma_0|\mathbf{h}|}{x_0^2 + \left(\Gamma_0 + \frac{|\mathbf{h}|}{2}\right)^2}, \quad (13)$$

where \mathbf{h} is the reciprocal-lattice vector corresponding to $00h$, $x_0 = K(x/L)$, K , the wave number, L , the camera length, and $\Gamma_0 = K\alpha$ is the normal component of k_0 to the crystal surface (see Fig. 9). Equation (13) tends to unity with the increase in x_0 . The observed trend, that the asymmetric profile of the H.K. line becomes noticeable with the increase in χ and finally results in the contrast reversal, is now understood as being due to the increase of the band term with the increase in χ .

The form of the transitional boundary or of the \mathbf{q} boundary defined in § 4 can also be deduced from (13). Let us assume that the transitional region on an H.K. line is the place corresponding to $b_B = c$ ($0 \leq c \leq 1$), and

that the coordinate of E in Fig. 9 ($\vec{DE} = \mathbf{q} = \mathbf{Q}_h$) is given as (x_0, y_0) . Since $2y_0 = 2\Gamma_0 - |\mathbf{h}|$, by eliminating $|\mathbf{h}|$ in (13) we obtain

$$x_0^2 + [y_0 + 2c\Gamma_0/(1-c)]^2 = 4c\Gamma_0^2/(1-c)^2. \quad (14)$$

Equation (14) determines the shape of the \mathbf{q} boundary, which is a circle with the centre at $[0, -2c\Gamma_0/(1-c)]$ and radius $2c\Gamma_0/(1-c)$ (Fig. 10). The shape of the transitional boundary and its movement with the specular spot as described in § 4 are qualitatively in agreement with those of this circle.

Fig. 11 shows the variation of b_B as a function of Γ_0 for $x_0 = 0$. With the increase in Γ_0 (accordingly, in α), b_B decreases first from unity at $\Gamma_0 = 0$ to zero at $\Gamma_0 = |\mathbf{h}|/2$,* and then monotonically increases tending again to unity. This variation is also in accordance with the trend experimentally observed for the intensity variation of the central part of an H.K. line with the change of the glancing angle.

7. Concluding remarks

The peculiarity of the H.K. lines compared with the ordinary Kikuchi lines in the Laue case is a combined result of the circumstance that only one tie-point is permitted on the dispersion surface in the Bragg case, and of the absorption effect.† In dealing with inelastic processes in a semi-infinite crystal, it is essential to take account of absorption (Miyake, Hayakawa & Miida, 1968); the scattering intensity J_0 otherwise diverges except for the range of $|W| < 1$. Actually, the intensity J_0 remains finite because of the factor $1/\mu$ contained in the function $S(\mathbf{Q}, \mathbf{Q}_h)$ etc., as in equation (9).

In the previous section the character of the H.K. lines has been discussed on the basis of (11) as well as the form of b_B given by (12), wherein the contribution of the background term in equation (6) to the line profile has been disregarded. It should be noted that this term for the Kikuchi pattern in a reflexion photograph from a semi-infinite absorbing crystal does, in contrast with that in a transmission photograph from a thin crystal, depend on W through the absorption coefficient μ given by (10). The background term in equation (6) is, in its magnitude, not always negligible compared with the other two terms, especially for the range $b_B \sim 1$. However, since the variation of $1/\mu$ with W is relatively smaller than that of $S(\mathbf{Q}_h, \mathbf{Q}_h)$ and $S(\mathbf{Q}, \mathbf{Q})$, the main feature of the calculated profiles of the H.K. lines and other theoretical conclusions are not substantially affected by the neglect of the background term.

It is worth noting that the simple theory presented

* The present theory is not valid at the condition $\Gamma_0 = |\mathbf{h}|/2$ for $x_0 = 0$, under which the specular spot overlaps the H.K. line $00h$ so that the initial state $|\psi_{k_0}^{\pm}\rangle$ is not a single plane wave.

† On this occasion, one of the present authors (T.K.) would like to make a correction to the previous paper (Kawamura *et al.*, 1973), that the interpretation given there of the origin of the contrast reversal of the H.K. lines should be replaced by the consideration extended in the present paper.

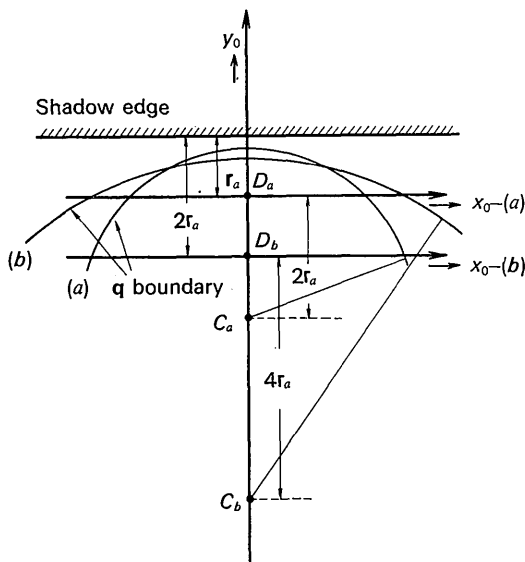


Fig. 10. Approximate shape of the \mathbf{q} boundary assuming $c = 0.5$ in equation (14). (a) for $\Gamma_0 = \Gamma_a$, (b) for $\Gamma_0 = 2\Gamma_a$. D_a and D_b are the direct spots in each case. The \mathbf{q} boundary is a circle, with the centre at $(0, -2\Gamma_0)$ and with radius $2/2\Gamma_0$. The coordinate origin is chosen at the direct spot in each case, and C_a and C_b are the centres of the circles in the cases of (a) and (b) respectively.

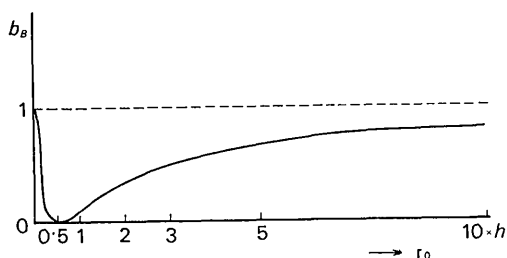


Fig. 11. The variation of b_B as a function of Γ_0 for $x_0 = 0$. b_B is almost equal to 0.5 at $\Gamma_0 = 3|\mathbf{h}|$.

above, in which only the single inelastic scattering of electrons is taken into account, is successful at least qualitatively in explaining the experimental features observed for the H.K. lines. This is probably because any inelastic process of the electron scattering contributing to formation of the H.K. lines can take place only at a small depth beneath the crystal surface as a result of the small extinction distance in the Bragg case, which is estimated to be of the order of ten Ångströms at most for lower-order H.K. lines from MgO.

Other simplifications assumed in the theory, such as those due to the two-wave approximation and the approximate forms of the structure factors for Kikuchi patterns, should be more refined for quantitative discussion. In this respect, however, more quantitative experimental data should be accumulated.

References

- ALAM, M. N., BLACKMAN, M. & PASHLEY, D. W. (1954). *Proc. Roy. Soc. A* **221**, 224–242.
- ARIH, T. (1973). *J. Phys. Soc. Japan*, **34**, 1297–1302.
- CHUKHOVSKII, F. N., ALEXANJAN, L. A. & PINSKER, Z. G. (1973). *Acta Cryst.* **A29**, 38–45.
- ISHIDA, K. (1970). *J. Phys. Soc. Japan*, **28**, 450–457.
- ISHIDA, K. (1971). *J. Phys. Soc. Japan*, **30**, 1439–1448.
- KAINUMA, Y. (1955). *Acta Cryst.* **8**, 247–257.
- KAWAMURA, T., ICHIKAWA, M. & GOLDSZTAUB, S. (1973). *Phys. Stat. Sol. (a)* **19**, 647–652.
- KOHLER, M. (1933). *Ann. Phys.* **18**, 265–287.
- MESSIAH, A. (1965). *Quantum Mechanics*. New York: John Wiley.
- MIYAKE, S., HAYAKAWA, K. & MIIDA, R. (1968). *Acta Cryst.* **A24**, 182–191.
- NAKAI, Y. (1970). *Acta Cryst.* **A26**, 459–460.
- OKAMOTO, K., ICHINOKAWA, T. & OHTSUKI, Y. H. (1971). *J. Phys. Soc. Japan*, **30**, 1690–1701.
- PFISTER, H. (1953). *Ann. Phys. Leipz.* **11**, 239–269.
- SHIONOHARA, K. & MATSUKAWA, K. (1933). *Sci. Papers Inst. Phys. Chem. Res. Tokyo*, **21**, 21–25.
- TAKAGI, S. (1958). *J. Phys. Soc. Japan*, **13**, 278–286, 287–296.
- WU, T. Y. & OHMURA, T. (1962). *Quantum Theory of Scattering*. New Jersey: Prentice-Hall.

Acta Cryst. (1975). **A31**, 38

Discrepancy Factors for use in Crystal Structure Analysis. II. Normalized Index \bar{R}_2 for Crystals with a Few Heavy Atoms in the Asymmetric Unit Belonging to the Triclinic, Monoclinic and Orthorhombic Systems*

BY V. PARTHASARATHI AND S. PARTHASARATHY

Centre of Advanced Study in Physics, University of Madras, Guindy Campus, Madras 600025, India

(Received 24 July 1974; accepted 27 July 1974)

Theoretical expressions for the normalized form of the discrepancy index R_2 of Wilson have been obtained for crystals containing heavy atoms of similar scattering power, with the heavy-atom part of the structure taken as the trial model. The results obtained are applicable for crystals belonging to 72 space groups of the triclinic, monoclinic and orthorhombic systems. Expressions for two limiting situations, namely complete relatedness and complete unrelatedness, have been tabulated for the commonly occurring cases corresponding to the number of heavy atoms in the asymmetric unit being one or two. Theoretical curves for this index as a function of the fractional heavy-atom contribution are also given for the various cases.

Introduction

Wilson (1969) suggested the discrepancy index R_2 (which is the ratio of the sum of the squares of the differences in the observed and calculated intensities over the various observed reflexions to the sum of the squares of the observed intensities) for use in crystal structure analysis, since it is the simplest index to manipulate theoretically. He has also considered the effect of a badly misplaced atom on this index.

Parthasarathy & Parthasarathi (1972) (hereafter abbreviated as PP, 1972) have worked out theoretical expressions of this index for crystals containing a few (*i.e.* 1 or 2) or many heavy atoms in the unit cell, and their final expressions (Table 1 of PP, 1972) are valid for triclinic space groups only. Since organic molecules crystallize more frequently in monoclinic or orthorhombic than in triclinic space groups, it would be useful to work out the values of this index* for these space groups corresponding to the commonly occur-

* Contribution No. 380 from the Centre of Advanced Study in Physics, University of Madras, Guindy Campus, Madras 600025, India.

* The theoretical evaluation of other possible types of discrepancy indices for space groups of higher symmetry seems to be too complicated to be carried out at present.